Performance Characterization and Remedy of Experimental $CuInGaSe_2$ Mini-Modules

Preprint

F.J. Pern, F. Yan, L. Mansfield, and S. Glynn
National Renewable Energy Laboratory

M. Rekow and R. Murison
ESI-PyroPhotonics Lasers, Inc.

Presented at the 37th IEEE Photovoltaic Specialists Conference (PVSC 37)
Seattle, Washington
June 19-24, 2011

Conference Paper
NREL/CP-5200-51812
July 2011

Contract No. DE-AC36-08GO28308

NOTICE

Available electronically at http://www.osti.gov/bridge

Available for a processing fee to U.S. Department of Energy
and its contractors, in paper, from:

U.S. Department of Energy
Office of Scientific and Technical Information

P.O. Box 62
Oak Ridge, TN 37831-0062
phone: 865.576.8401
fax: 865.576.5728
email: mailto:reports@adonis.osti.gov

Available for sale to the public, in paper, from:

U.S. Department of Commerce
National Technical Information Service
5285 Port Royal Road
Springfield, VA 22161
phone: 800.553.6847
fax: 703.605.6900
email: orders@ntis.fedworld.gov
online ordering: http://www.ntis.gov/help/ordermethods.aspx

Cover Photos: (left to right) PIX 16416, PIX 17423, PIX 16560, PIX 17613, PIX 17436, PIX 17721

Printed on paper containing at least 50% wastepaper, including 10% post consumer waste.

PERFORMANCE CHARACTERIZATION AND REMEDY OF EXPERIMENTAL $CuInGaSe_2$ MINI-MODULES

F. J. Pern[1], F. Yan[1], L. Mansfield[1], S. Glynn[1], M. Rekow[2], and R. Murison[2]
[1] National Center for Photovoltaics, National Renewable Energy Laboratory, 1617 Cole Blvd., Golden, CO 80401, USA
[2] ESI-PyroPhotonics Lasers, Inc., 1275 Kesmark, Dollard-des-Ormeaux, QC Canada H9B 3J1

ABSTRACT

We employed current-voltage (I-V), quantum efficiency (QE), photoluminescence (PL), electroluminescence (EL), lock-in thermography (LIT), and (electrochemical) impedance spectroscopy (ECIS) to complementarily characterize the performance and remedy for two pairs of experimental $CuInGaSe_2$ (CIGS) mini-modules. One pair had the three scribe-lines (P1/P2/P3) done by a single pulse-programmable laser, and the other had the P2/P3 lines by mechanical scribe. Localized QE measurements for each cell strip on all four mini-modules showed non-uniform distributions that correlated well with the presence of performance-degrading strips or spots revealed by PL, EL, and LIT imaging. Performance of the all-laser-scribed mini-modules improved significantly by adding a thicker Al-doped ZnO layer and reworking the P3 line. The efficiency on one of the all-laser-scribed mini-modules increased notably from 7.80% to 8.56% after the performance-degrading spots on the side regions along the cell array were isolated by manual scribes.

INTRODUCTION

One of the advantages in thin-film PV technologies is the use of monolithic integration for fabricating modules; these modules' performance can be affected by the quality of absorber, cell components, and scribe lines. The conventional scribing process for monolithically integrated CIGS modules in production lines typically uses a laser for Mo removal (P1) followed by mechanical stylus for P2 and P3 scribes [1–5]. As it is well known, mechanical scribing can cause potential tearing of coated layers and a zig-zag feature of the scribe lines; additionally, the line-to-line spacing can not be very narrow. Therefore, all-laser scribing for the three scribe lines is highly attractive. Extensive studies on laser scribing for component layers of thin-film solar cells using different wavelength and pulse laser systems were conducted previously by Compaan and coworkers [6,7]. In practice, use of a single laser and single wavelength will greatly simplify the processing. To address these issues, the collaboration between NREL and PyroPhotonics has investigated and reported for the first time the use of a single pulse-programmable laser with a single wavelength (1064 nm) to achieve successful scribing of all three P1, P2, and P3 lines [8-10]. The technical details were described in ref. [10]. Good-quality scribe lines were demonstrated on CIGS mini-modules made on soda lime glass substrates [8]. Previously, we also demonstrated that the electrical performance of the pair of all-laser-scribed mini-modules could be remedied (improved) by P3 rework, after the thickness of the Al-doped ZnO (AZO) window layer was increased from an initial 0.12 μm to 0.50 μm to decrease the sheet resistance. The results were comparable with a pair of P2/P3 mechanically scribed mini-modules with an initial 0.50 μm AZO [9,10]. However, due to time constraint, the four mini-modules were not thoroughly characterized prior to those reports given in ref. [8-10]. This paper describes our continued efforts at NREL to seek and employ useful characterization methods to better understand and identify the performance-limiting factors as well as to evaluate and implement simple remedy methods to mitigate those factors to improve performance. As detailed below, the results indicate that PL, EL, LIT, and localized QE measurements are highly complementary in identifying the degrading spots or regions that directly affect the performance of individual cell strip on the mini-modules, and that simple manual scribes can be used to isolate off those spots or regions, resulting in significant improvements in efficiency. ECIS analysis renders further understanding of the electrical characteristics of the mini-modules before and after remedy. This paper presents a summary of results from recent work combined with some of previous studies.

EXPERIMENTAL

Details of the collaborated work to fabricate the mini-modules and their performance prior to recent work were described previously in ref. [8-10]. The mini-modules were characterized by I-V measurements for the entire working area using an Optical Radiation Corp.'s Solar Simulator 1000. Localized QE on each cell strip was measured with a custom-built QE system using a small, narrow probing light beam. Using also a custom-built system for PL (and EL) imaging, 810 nm laser diodes were used as the excitation source at a condition close to one-sun intensity, with RG1000 Schott glass filters mounted on the camera lens to sufficiently attenuate the reflected laser light. The PL signal was collected by a cooled silicon charge-coupled device (CCD) camera. The EL imaging was conducted on the same setup by driving forward-bias current through the test cells. In this case, the long-pass filters on the camera were removed. Illuminated lock-in thermography (LIT) was also employed initially but was not available in later stage due to maintenance repair. To test the possibility and effectiveness of remedy processing, either the 1064-nm laser or a sharp diamond-tipped scribe was used to remove or isolate the "defective" spots or

regions, as identified by PL and EL (and LIT), on the two all-laser-scribed mini-modules. The mini-modules' performance was then re-measured, followed by PL and EL imaging. The mini-modules were also examined in the dark with an ECIS system comprised of an SI 1260 impedance/gain-phase analyzer and an SI 1286 electrochemical interface from Schlumberger Technologies operated with ZPlot and ZView software from Scribner Associates.

RESULTS AND DISCUSSION

Characterization by PL, EL, and LIT imaging

Figure 1 shows the room-light, PL, EL, and LIT images for the all-laser-scribed mini-module C2681 at its initial stage with 0.12 μm AZO. The room-light image in Fig. 1(a) shows apparently (visibly) uniform appearance over the entire mini-module except for a visible white spot close to the left edge of the cell strip #9 (as marked in Fig. 1(a) from top down). However, this white spot, likely produced by the "spitting" during CIGS film deposition, caused a large black area on the PL image in Fig. 1(b), produced a large white spot in LIT (Fig. 1(d)), and rendered the entire cell strip EL-inactive, as seen in Fig. 1 (c). In addition, PL, EL and LIT imaging revealed many more recombination-active spots as seen in Fig. 1 (b-d). These recombination-active spots, large or small, were also observed on three other mini-modules, indicating the presence of inherent deficiency in the aged vacuum thermal co-evaporation system used for the CIGS film growth.

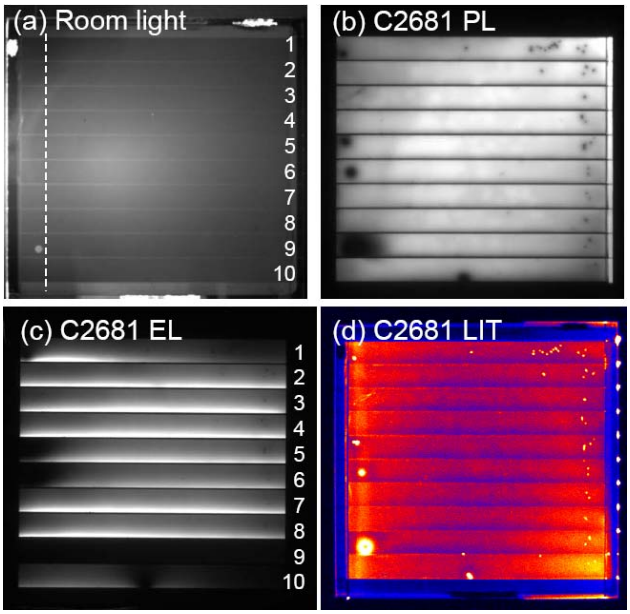

Figure 1 (a) Room-light, (b) PL, (c) EL, and (d) LIT images for the all-laser-scribed mini-module, C2681, with 0.12 μm AZO.

Performance Remedy

By AZO thickness increase and P3 rework. The two all-laser-scribed mini-modules, C2681 and C2684, with an initial 0.12-μm AZO showed poor efficiency at 5.31% and 4.08% due to high series resistance (Rs = 114 and 128 ohm-cm^2), low shunt resistance (Rsh = 503 and 280 ohm-cm^2) and fill factor (FF = 34.3% and 29.6%), respectively. Compared with the ~16% efficiency and >90% external quantum efficiency (EQE) at 750 nm of small-size (0.42-cm^2) cells on a control, the poor performance was obviously introduced in part by the 0.12-μm AZO layer, which was insufficient for the 6.5-mm cell width [8]. The low Rsh indicates the presence of shunting however, possibly introduced by scribing. To utilize the high precision and repeatability of laser scribing and the low extent of damaging along the two sides of the scribed line [8] as well as to examine the possibility of remedying the poor performance, another layer of 0.38-μm AZO was added and the P3 scribe line reworked on both mini-modules. The width of the reworked scribe lines remained very narrow (compare Fig. 2(a and c) with Fig. 1(b and c)). In comparison, the scribe lines made by mechanical scribing on two other mini-modules with 0.50-μm AZO were substantially wider as revealed by the dark lines in PL and EL images (not shown). Additionally, a narrow strip on the left side of C2681, where the visible spot was located, was also ablated off by the laser, as indicated by the white dash line in Fig. 1(a). PL and EL imaging in Fig. 2(a and c) revealed the changes: the four black dots and area seen on cell strips #1, 5, 6, and 9 in Fig. 1(b and c) are no longer present. Cell strip #1 became dimmed in PL

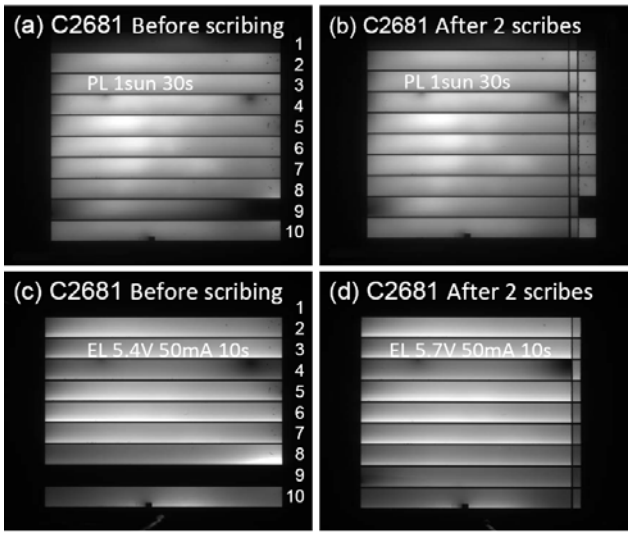

Figure 2 (a, b) PL and (c, d) EL images for the mini-module C2681 P3-reworked with 0.50 μm AZO before and after two manual scribes on the right side to isolate the regions having numerous black dots and a large spot on cell strip #9. A narrow strip on the mini-module's left side was previously ablated off with laser as indicated by the dashed white line in Fig. 1(a).

and EL, as seen in Fig. 2(a and c), however, suggesting a shorting problem likely caused by unsatisfactory P3 rework. Cell strip #9 also remained EL-inactive, indicating the presence of "other" performance-degrading area, which is clearly identified to be on the right side of the cell strip as seen in Fig. 2(a). The performance of P3-reworked C2681 and C2684 mini-modules with 0.50-μm AZO were improved substantially, as reported previously in ref. [8,9] and also given in the top half of Table 1 below.

Without further investigation one would attribute the efficiency improvement from I-V measurements to the reduced sheet resistance from thicker AZO and the removal of the recombination spots and regions on the left edge. However, results of subsequent localized EQE measurements for every individual cell strip (a total of 10) on C2681 and C2684 showed that some cell strips had improved (e.g., strips #5 and #8) and some became worse than before (strips #2 and #10), indicating the potential shortcoming of *manual* P3 rework. The EQE plots in Fig. 3 illustrate the small-to-significant improvement for cell strips #5 and #8 on the two all-laser-scribed mini-modules. The QE curves also show the spectral changes due to AZO thickness increase. The non-uniform changes in QE were further confirmed with PL and EL imaging, as given in Fig. 2 above.

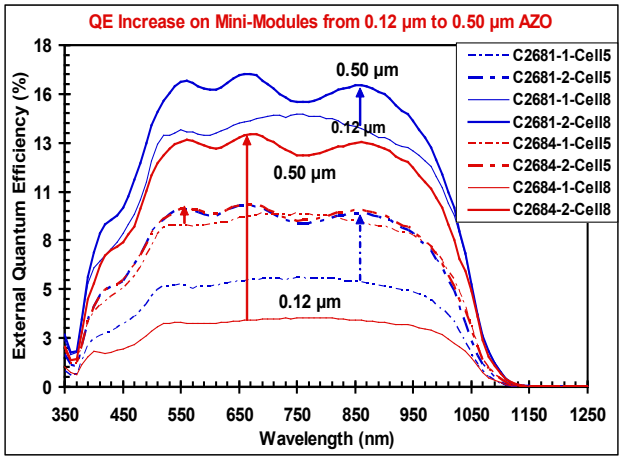

Figure 3 External quantum efficiency (EQE) spectra measured for cell strips #5 and #8 on the two all-laser-scribed mini-modules before and after addition of a thicker AZO and P3 rework.

By manual scribes to isolate recombination-active areas. In order to test the effectiveness of further performance improvement, the right edge with numerous small black dots seen in Figs. 1 and 2 was isolated by manually scribing twice (sequentially) with a sharp diamond-tipped scribe. The two scribes are seen as the two linear black lines in the PL and EL images in Fig. 2 (b and d). After each scribe, the mini-module C2681 was I-V and QE measured. The two scribes resulted in further efficiency improvements from 7.80% to 8.38% and 8.56%, whereas the cell strip #9 now became PL- and EL-active, as seen in Fig. 2 (a vs. b) and (c vs. d). The "other" performance-degrading area is seen now located on the right edge of the cell strip. However, the cell strip #1 remained inactive since the P3 rework as indicated by QE, PL, and EL imaging and could not be recovered by the two manual scribes; this indicates the presence of a serious shorting that has yet to be identified and remedied with more work. For the second all-laser-scribed mini-module C2684, similar manual scribe was conducted once, resulting in a small efficiency improvement (Table 1). No manual scribes were performed on the two mechanically-scribed mini-modules, C2682 and C2683, because the recombination-active black spots were located mostly in the central regions of the mini-module squares (not shown).

Performance non-uniformity characterized by localized QE measurements

Figure 4 compares the EQE values at six wavelengths (450, 550, 650, 750, 850, and 950 nm) for the mini-module C2681 at its initial condition (top) and at its final state after all three isolation treatments (bottom). The performance non-uniformity is clearly reflected by the uneven QE response of each individual cell strip on the mini-module C2681. Similar results are also obtained on three other mini-modules. The effect of adding a thicker AZO layer, P3 rework, and two manual scribes is reflected by the changes in individual QE response (top vs. bottom). The QE responses correlate qualitatively with the PL and EL intensity seen in Figs. 1 and 2 for the C2681 at its initial state. However, for the mini-module at its final state, as

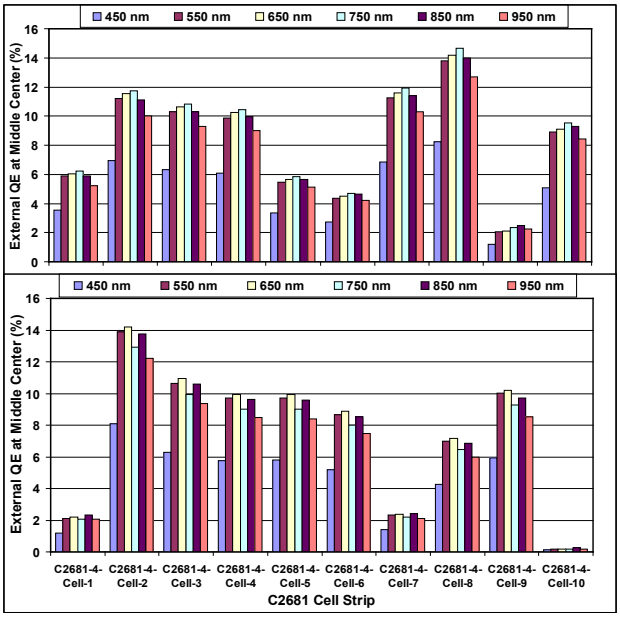

Figure 4 EQE at six wavelengths for the 10 cell strips on C2681 mini-module at its initial condition with 0.12 um AZO (top) and at its final state after addition of a thicker AZO layer, P3 rework, and two manual scribes (bottom). See text for details.

Table 1 I-V Parameters for Four Mini-Modules with or without Isolation Scribes

Mini-Module File ID	Total AZO (μm)	Film/Edges Reworked	Cell Strip Area (cm^2)	Voc (V)	Jsc (mA/cm^2)	FF (%)	Eff. (%)	Rs (ohm-cm2)	Rsh (ohm-cm2)	# Cell Strips
(a) All-Laser-Scribed										
C2681-1	0.12	No	4.49	5.742	26.97	34.30	5.31	113.6	503.4	10
C2681-2	0.50	P3 & Isolate-1	3.90	5.846	26.74	46.32	7.24	81.9	697.2	
C2681-2N		(new meas.)	3.90	5.758	28.23	48.00	7.80	62.2	714.0	
C2681-3N		Manual scribe-1	3.58	5.810	28.50	50.58	8.38	57.6	728.4	
C2681-4		Manual scribe-2	3.45	5.795	29.28	50.46	8.56	60.0	723.0	
C2684-1	0.12	No	4.49	4.979	27.61	29.65	4.08	128.0	280.5	10
C2684-2	0.50	P3	4.23	5.975	26.76	51.93	8.30	48.1	726.0	
C2684-2N		(new meas.)	4.23	5.998	28.20	54.10	9.15	43.2	854.3	
C2684-3N		Manual scribe-1	3.74	6.001	28.22	54.18	9.18	48.7	832.7	
(b) P1 Laser + P2/P3 Mechanical										
C2682-2	0.50	Left half isolated	2.78	5.811	25.16	51.18	7.48	49.2	999.8	10
C2682-2N		(new meas.)	2.78	5.752	26.59	49.59	7.59	54.5	890.7	
C2683-2	0.50	No	4.06	5.458	25.19	48.22	6.63	50.3	761.1	9
C2683-2N		(new meas.)	4.06	5.412	26.25	45.69	6.49	59.9	520.8	

shown in Fig. 2 (b and d), the correlation is lost particularly in the region from cell strip #7 to #10. The revival of cell strip #9 upon scribe isolation is evident by the large increase in QE response, but the cell strips #7, 8 and 10 show large reductions in QE. While the exact cause is not readily determined, it is likely that there is some level of QE current leakage on the cell strips introduced by the second manual scribe. This reasoning is evident by the still EL-active narrow strip between the two manual scribe lines seen in Fig. 2(d), which should have become EL inactive (dark) if the scribe had completely broken all electrical connections as the first manual scribe did.

The I-V parameters for the four mini-modules at its initial state and after remedy treatments are summarized in Table 1 for comparison. The subsequent beneficial effects of isolating off the performance-degrading areas, i.e., P3 rework with adding a thicker AZO followed by one or two manual scribes, as indicated in the "film/edge reworked" column and by the number after the mini-module ID, are shown for the two all-laser–scribed mini-modules, C2681 and C2684. One interesting observation is that, except for C2683, the other three mini-modules showed higher efficiency after having been stored in a N_2-purged drybox for nearly eight months and I-V re-measured prior to manual scribes, e.g., a 7.7% increase in C2681-2N vs. C2681-2, and a 10.2% increase in C2684-2N vs. C2684-2, where N stands for new measurement. (It should be noted that the light intensity of solar simulator set for the Si reference cell was adjusted slightly higher by ~4.5% in between.) The corresponding series resistance Rs decreased and shunt resistance Rsh increased on both all-laser–scribed mini-modules, but the changes in Rs and Rsh were reversed on the mechanically scribed pair. The reason is not clear, although without any supporting evidence, one inclines to suspect there was some sort of material settlement during the storage period.

Impedance spectroscopy analysis

(Electrochemical) impedance spectroscopy (IS or ECIS as used here) has been applied to characterize various solar cells including Si, dye-sensitized, and CIGS solar cells [11-17]. The four mini-modules were also characterized by ECIS using a 10-mV AC modulation amplitude without bias sweeping from 1M Hz to 1 Hz in the dark. No measurements were available for the all-laser-scribed mini-modules at its initial state with 0.12 μm AZO. Figure 5 shows the complex plane plots (imaginary Z" vs. real Z') for the four mini-modules. Essentially, all four CIGS mini-modules can be represented by a simple "Rs' + (Rp // C)" equivalent circuit, where Rs' is the series resistance for contacts and bulk, Rp the recombination/diffusion resistance, and C the depletion/diffusion capacitance of the solar cells in parallel to Rp [11-17]. Diffusion resistance and capacitance for CIGS solar cells or mini-

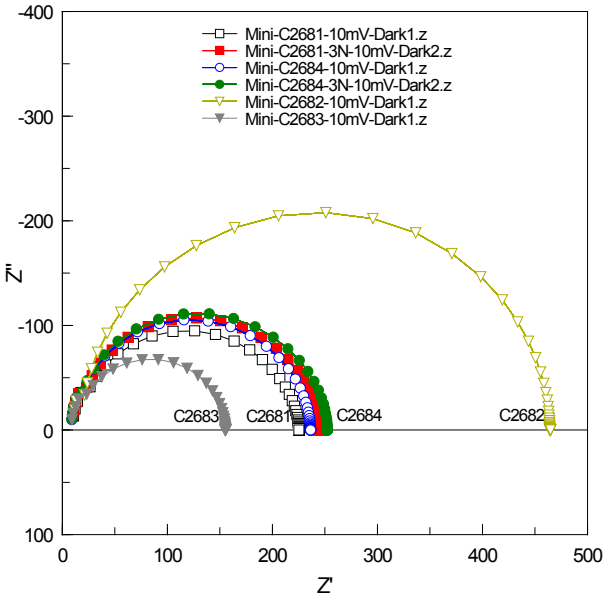

Figure 5 Complex plane plots for the four mini-modules, ID indicated next to the curves, with or without the manual scribes described in the text.

modules is insignificant here. From the intercepts of the semicircle on the real Z' axis, Rs' and Rp values can be easily obtained. C can be derived from curve fitting with the ZView software.

Table 2 summarizes the Rs and Rsh (in ohm-cm^2) from light I-V measurements (shown in Table 1 too) , Rs' and Rp (in ohm) from ECIS measurements at 1 Hz and 1M Hz and curve fitting data, and effective minority-carrier lifetime (or time constant, in second) calculated from the product of Rp and C (in farad). The Rs' and Rp values derived from curve fitting are generally close to the resistance values obtained directly for Z' at 1 Hz and 1M Hz, respectively. Curve fitting results for all data show the mini-modules are better fitted with an equivalent circuit having a *depressed* "constant phase element (CPE-P)" factor (Table 2) [17,18]. The CPE-P, typically between 0.9 and 1.0 (1.0 for an ideal case of capacitor), can be viewed as an indicator of the presence of interface or surface states on rough or porous surfaces [17,18]. The relatively high contact/bulk resistance Rs' and low recombination resistance Rp from dark ECIS measurements correspond to the high series resistance (Rs) and low shunt resistance (Rsh) from light I-V measurements, inevitably resulting in low fill factor (FF) and thus low performance efficiency of the four mini-modules. Upon manual scribes, the two laser-scribed mini-modules exhibit a small increase in the resistance of Z' at 1 Hz, or Rp from curve fitting. The order of the performance efficiency of the mini-modules, which is C2684 (9.18%) > C2681 (8.56%) > C2682 (7.56%) > C2683 (6.49%) in Table 1, correlates somewhat better with the inverse order of contact/bulk resistance Rs', which is C2684 (10.2 ohms) < C2681 (10.6) < C2683 (11.1) < C2682 (18.4) in Table 2, rather with the order of effective minority-carrier lifetime (or time constant, the product of Rp*C [13]), which gives C2683 > C2684 > C2681 > C2682. More work with better scribe-isolation quality and higher performance CIGS mini-modules will be needed in order to establish a good correlation between the PV performance parameters and the electrical parameters from ECIS measurements [19].

CONCLUSIONS

We have shown that PL and EL imaging (and LIT when available) are complementary with I-V and localized QE measurements in characterizing the performance of the experimental mini-modules. The PL and EL imaging are very useful in identifying the presence and location of performance-degrading spots/regions, where remedy treatment may be rendered – if physically practical – to improve performance efficiency. The ECIS analysis is sensitive to detect changes in electrical parameters of the mini-modules and also complementary to the I-V measurements. A prompt application from this study has been to employ the rapid PL imaging to detect the poor regions on the CdS-coated CIGS absorber and isolate them in advance from making devices over those areas.

ACKNOWLEDGEMENTS

We thank M. Contreras, T. Gessert, and R. Noufi for the support of this collaboration work and S. Johnston for the support of PL, EL, and LIT imaging work by F. Yan. This work was performed at the National Center for Photovoltaics under DOE Contract No. DE-AC36-08GO28308 with the National Renewable Energy Laboratory.

REFERENCES

[1] M. Powalla and B. Dimmler, "Process Development of High Performance CIGS Modules for Mass Production," *Thin Solid Films*, **387,** 2001, pp. 251–256.

[2] M. Powalla, D. Hariskos, E. Lotter, M. Oertel, J. Springer, D. Stellbogen, B. Dimmler, and R. Schäffler, "Large-Area CIGS Modules: Processes and Properties," *Thin Solid Films*, **431**-**432,** 2003, pp. 523–533.

[3] J. Palm, W. Stetter, S. Visbeck, T. Niessen, M. Furfanger, H. Vogt, J. Baumbach, H. Calwer, V. Probst, and F. Karg, "Pilot-Line CIGSSE Power Modules Processing and Qualification at Shell Solar," *Proc. 20th EuPVSEC*, June 6–10, 2005, Barcelona, Spain.

Table 2 (Electrochemical) Impedance Spectroscopy Analysis of Mini-Modules with or without Manual Scribes

				From LIV Meas.		From ECIS Meas.		From Curve Fitting				
Mini-Module ID - State	AZO (μm)	P1-P3 Scribe Method	Manual Scribe #	Rs (ohm-cm)	Rsh (ohm-cm)	Z' (1M Hz) (ohm)	Z' (1 Hz) (ohm)	Rs' (ohm)	Rp (ohm)	C (F) or CPE-T	CPE-P	Lifetime (Rp*C) (s)
C2681-2	0.50	All Laser	0	62.2	714.0	10.8	225.4	10.7	213.9	1.849E-08	0.945	3.954E-06
C2681-4	0.50	All Laser	2	60.0	723.0	10.0	244.9	10.6	233.1	1.335E-08	0.970	3.112E-06
C2684-2	0.50	All Laser	0	43.2	854.3	12.8	236.1	10.9	224.7	1.288E-08	0.981	2.895E-06
C2684-3N	0.50	All Laser	1	48.7	832.7	9.1	252.2	10.2	240.8	1.400E-08	0.974	3.371E-06
C2682-2N	0.50	P1 Laser, P2 & P3 Mechanical	0	54.5	890.7	11.9	465.8	18.4	445.8	9.065E-09	0.977	4.040E-06
C2683-2N	0.50	P1 Laser, P2 & P3 Mechanical	0	50.3	761.1	9.2	155.9	11.1	144.3	1.269E-08	0.983	1.831E-06

[4] M. Powalla, M. Cemernjak, J. Eberhardt, F. Kessler, R. Kniese, H.D. Mohring, and B. Dimmler, "Large-Area CIGS Modules: Pilot Line Production and New Developments," *Solar Energy Materials and Solar Cells*, **90,** 2006, pp. 3158–3164.

[5] B. Dimmler and R. Wächter, "Manufacturing and Application of CIS Solar Modules," *Thin Solid Films*, **515,** 2007, pp. 5973-5978.

[6] A.D. Compaan, I. Matulionis, and S. Nakade, "Optimization of Laser Scribing for Thin-Film PV Modules," Final Technical Progress Report, 12 April 1995 – 11 October 1997. The University of Toledo, Toledo, Ohio. NREL/SR-520-24842, June 1998.

[7] A.D. Compaan (2000, Jan. 1), "Photovoltaics: Laser Scribing Creates Monolithic Thin-Film Arrays," retrieved from Laser Focus World, http://www.laserfocusworld.com/articles/58212.

[8] F.J. Pern, L. Mansfield, S. Glynn, B. To, C. DeHart, S. Nikumb, C. Dinkel, M. Rekow, R. Murison, T. Panarello, and C. Dunsky, "All-Laser Scribing for Thin-Film Cuingase$_2$ Solar Cells," *Proc. 35th IEEE PVSC*, June 20-25, 2010, Honolulu, Hawaii.

[9] R. Murison, C. Dunsky, M. Rekow, C. Dinkel, F.J. Pern, L. Mansfield, T. Panarello, and S. Nikumb, "CIGS P1, P2, and P3 Laser Scribing With An Innovative Fiber Laser," *Proc. 35th IEEE PVSC*, June 20-25, 2010, Honolulu, Hawaii.

[10] M. Rekow, R. Murison, C. Dunsky, C. Dinkel, J. Pern, L. Mansfield, T. Panarello, and S. Nikumb, "CIGS P1, P2, P3 Scribing Processes using a Pulse Programmable Industrial Fiber Laser," *Proc. of 25th EU PVSEC/WCPEC-5*, Sept. 6-10, 2010, Valencia, Spain.

[11] M. S. Suresh, "Measurement of Solar Cell Parameters using Impedance Spectroscopy," Solar Energy Materials and Solar Cells, **43**, 1996, pp. 21-28.

[12] J. Bisquert, "Theory of the Impedance of Electron Diffusion and Recombination in a Thin Layer," J. *Phys. Chem. B,* **106**, 2002, pp. 325-333.

[13] J. Bisquert, "Impedance Spectroscopy Applied on Solar Cells," a presentation at the Nordic Workshop on Solar Electricity, Sonnerupgaard Gods, Denmark, 27-29 April 2004.

[14] I. Mora-Sero, G. Garcia-Belmonte, P. P. Boix, M. A. Vazquez, and J. Bisquert, "Impedance Spectroscopy Characterisation of Highly Efficient Silicon Solar Cells under Different Light Illumination Intensities," *Energy Environ. Sci.*, **2**, 2009, pp. 678–686.

[15] H. Bayhan and A. S. Kavasoglu, "Admittance and Impedance Spectroscopy on Cu(In,Ga)Se$_2$ Solar Cells, *Turk J. Phys.* **27**, 2003, pp. 529-535.

[16] H. Bayhan and A. S. Kavasoglu, "Study of CdS/Cu(In,Ga)Se$_2$ Heterojunction interface Using Admittance and Impedance Spectroscopy," *Solar Energy*, **80**, 2006, pp. 1160-1164.

[17] "*Impedance Spectroscopy – Emphasizing Solid Sate Materials and Systems*," J. Ross MacDonald ed., John Wiley & Sons, New York, 1987. See "Constant Phase Element" in Chapters 1 and 2.

[18] Help menu on equivalent circuits, instant curve fitting function and constant phase element in the ZView program (ver. 3.2c) from Scribner Associates, Inc.

[19] F. Fabregat-Santiago, J. Bisquert, E. Palomares, L. Otero, D. Kuang, S. M. Zakeeruddin, and M. Graetzel, "Correlation between Photovoltaic Performance and Impedance Spectroscopy of Dye-Sensitized Solar Cells Based on Ionic Liquids," *J. Phys. Chem. C,* **111**, 2007, pp. 6550-6560.